Optimum Activity of the Phosphofructokinase from *Ascaris suum* Requires More Than One Metal Ion†

Grant E. Gibson,‡,⊥ Ben G. Harris,‡ and Paul F. Cook*,§

Department of Molecular Biology and Immunology, University of North Texas Health Science Center at Fort Worth, 3500 Camp Bowie Boulevard, Fort Worth, Texas 76107, and Department of Chemistry and Biochemistry, University of Oklahoma, 620 Parrington Oval, Norman, Oklahoma 73019

Received October 26, 2005; Revised Manuscript Received December 12, 2005

ABSTRACT: Phosphofructokinase (PFK) catalyzes the phosphorylation of fructose 6-phosphate (F6P) to give fructose 1,6-bisphosphate (FBP) using MgATP as the phosphoryl donor. As the concentration of Mg^{2+} increases above the concentration needed to generate the MgATP chelate complex, a 15-fold increase in the initial rate was observed at low MgATP. The effect of Mg^{2+} is limited to V/K_{MgATP}, and initial rate studies indicate an equilibrium-ordered addition of Mg^{2+} before MgATP. Isotope partitioning of the dPFK:MgATP* complex indicates a random addition of MgATP and F6P at low Mg^{2+}, with the rate of release of MgATP from the central E:MgATP:F6P complex 4-fold faster than the net rate constant for catalysis. This can be contrasted with the ordered addition of MgATP prior to F6P at high Mg^{2+}. The addition of fructose 2,6-bisphosphate ($F26P_2$) has no effect on the mechanism at low Mg^{2+}, with the exception of a 4-fold increase in the affinity of the enzyme for F6P. At high Mg^{2+}, $F26P_2$ causes the kinetic mechanism to become random with respect to MgATP and F6P and with MgATP released from the central complex half as fast as the net rate constant for catalysis. The latter is in agreement with previous studies [Gibson, G. E., Harris, B. G., and Cook, P. F. (1996) *Biochemistry 35*, 5451−5457]. The overall effect of Mg^{2+} is a decrease in the rate of release of MgATP from the E:MgATP:F6P complex, independent of the concentration of $F26P_2$.

Phosphofructokinase (PFK)[1] catalyzes the phosphorylation of the 1-hydroxyl of fructose 6-phosphate (F6P) to give fructose 1,6-bisphosphate (FBP). In the parasitic nematode *Ascaris suum*, which has an anaerobic metabolism, the PFK reaction determines the flux through the glycolytic pathway, which ends with the production of L-malate. The PFK is highly regulated by small molecule effectors. Inhibition by ATP is observed at high concentrations as a result of binding to an allosteric site stabilizing a T state, while adenosine 5′-monophosphate (AMP) and fructose 2,6-bisphosphate ($F26P_2$) are activators binding to separate allosteric sites stabilizing an R state (*2*). Allosteric inhibition by ATP can be essentially eliminated by covalent modification of the ATP inhibitory site by diethylpyrocarbonate in the presence of high concentrations of F6P, generating a form of the enzyme termed dPFK, which is still activated by AMP and $F26P_2$ (*3*). In addition, a T state of the enzyme can be stabilized by covalent modification of the ATP inhibitory site with 2′,3′-dialdehyde ATP, giving an enzyme form termed oPFK (*4*). Although the enzyme exhibits a sigmoid saturation curve for F6P at pH values lower than 7.5, the curve becomes noncooperative at pH 8, likely a result of titrating the imidazole in the ATP inhibitory site (*5*).

The kinetic mechanism of the native form of the *A. suum* PFK at pH 8 and the dPFK at pH 6.8 has been studied in the absence and presence of the allosteric activator $F26P_2$ (*6*). The mechanism is steady-state-ordered in the absence of $F26P_2$, with MgATP adding prior to F6P and rapid release of FBP and MgADP in that order. $F26P_2$ is known to increase the affinity of the enzyme for F6P, with no effect on K_{iMgATP}, K_{MgATP}, or V (*7*). Isotope partitioning data corroborate the proposed kinetic mechanism and indicate that the mechanism becomes random in the presence of $F26P_2$, with MgATP dissociating from the E:MgATP:F6P central complex (*1*).

During the course of the above studies, which were all carried out at 8 mM Mg^{2+}, an increase in the initial rate was observed under conditions where the Mg^{2+} was increased above the concentration needed to generate the MgATP chelate complex. To determine whether more than one Mg^{2+} was required for optimum activity of PFK, initial rate and isotope partitioning studies have been carried out as a function of Mg^{2+} in the absence and presence of $F26P_2$. Data indicate that the kinetic mechanism changes from ordered

† This work was supported by a grant from the National Science Foundation to P.F.C. (MCB 009127), grants from the National Institutes of Health (AI 24155) and the Robert A. Welch Foundation to B.G.H. (BK 1309), and from the Grayce B. Kerr endowment to the University of Oklahoma to support the research of P.F.C.

* To whom correspondence should be addressed. Telephone: 405-325-4581. Fax: 405-325-7182. E-mail: pcook@chemdept.chem.ou.edu.

‡ University of North Texas Health Science Center at Fort Worth.

⊥ Current address: Luminex, 12212 Technology Blvd., Austin, TX 78727.

§ University of Oklahoma.

[1] Abbreviations: PFK, phosphofructokinase; oPFK, phosphofructokinase covalently modified by 2′,3′-dialdehyde ATP at the ATP inhibitory site; dPFK, phosphofructokinase covalently modified by diethylpyrocarbonate at the $F26P_2$ activator site; F6P, fructose 6-phosphate; $F26P_2$, fructose 2,6-bisphosphate; FBP, fructose 1,6-bisphosphate; BME, β-mercaptoethanol, PEP, phosphoenolpyruvate; EDTA, ethylenediamine tetraacetate; DEPC, diethylpyrocarbonate; NADH, reduced form of nicotinamide adenine dinucleotide; AMP, adenosine 5′-monophosphate.

10.1021/bi052191u CCC: $33.50
Published on Web 01/28/2006

to random as the Mg^{2+} concentration decreases. In the presence of $F26P_2$, the mechanism also becomes random as a result of an increase in the affinity of F6P (*1*), but Mg^{2+} still increases the affinity for MgATP at saturating $F26P_2$.

MATERIALS AND METHODS

Chemicals. [γ-^{32}P]ATP was purchased from ICN Radiochemicals. All other chemicals and enzymes were purchased from Sigma and used without further purification.

Purification of A. suum PFK. PFK from *A. suum* was purified according to the method of Allen et al. (*8*) with the exception of the addition of the protease inhibitors aprotinin (10 mg/L), trypsin inhibitor (20 mg/L), and phenylmethylsulfonyl fluoride (1 mM) to the crude extract and the DEAE-Sephacel eluate. The purified enzyme had a final specific activity of approximately 43 units/mg. The enzyme was stored in 50 mM KH_2PO_4 buffer at pH 7.5 with 2% glycerol and 10 mM β-mercatoethanol (BME). For initial velocity experiments, the enzyme was diluted with the same storage buffer to approximately 5 units/mL. For isotope partitioning experiments, the enzyme was concentrated to approximately 500 units/mL using an Amicon conical membrane centrifuge apparatus with a molecular-weight cutoff of 30 000.

Chemical Modification of Native PFK. The dPFK was prepared according to the method of Rao et al. (*3*), giving a final specific activity of 30 units/mg. The dPFK was stored in 50 mM KH_2PO_4 buffer at pH 6.8 with 2% glycerol and 10 mM BME. The concentration of the dPFK in initial velocity and isotope partitioning experiments was the same as for the native enzyme. The protein concentration of dPFK was determined by the method of Bradford (*9*), with bovine serum albumin as a standard.

Initial Velocity Studies. In the direction of phosphorylation of F6P, the production of FBP was coupled to the adolase/triosephosphate isomerase/α-glycerol phosphate dehydrogenase reactions and monitoring the disappearance of the reduced form of nicotinamide adenine dinucleotide (NADH) at 340 nm. A typical 1 mL reaction mixture contained 100 mM imidazole-HCl at pH 6.8, 8 mM $MgCl_2$, 14 units of aldolase, 34 units of triosephosphate isomerase, 4 units of α-glycerolphosphate dehydrogenase, 0.2 mM NADH, ATP and F6P as indicated, and 20 milliunits of PFK. MgADP formation was coupled to the pyruvate kinase−lactate dehydrogenase reactions, and a typical 1 mL reaction mixture contained 100 mM imidazole-HCl at pH 6.8, 8 mM $MgCl_2$, 3 units of pyruvate kinase, 3 units of lactate dehydrogenase, 100 mM KCl, 0.2 mM NADH, 0.2 mM phosphoenolpyruvate (PEP), ATP and F6P as indicated, and 20 milliunits of PFK. In initial velocity and inhibition experiments, a double-coupled assay was used, which monitors the production of both FBP and MgADP in the same 1 mL cuvette (*1*). The double-coupled assay gives greater sensitivity than either assay alone, avoids product inhibition by removing both products, and gives longer linear time courses by recycling ATP. All assays were initiated by the addition of PFK. The initial rate was a linear function of the dPFK concentration at all Mg^{2+} concentrations used. In addition, the initial rate is constant to an ionic strength of >0.25.

Initial velocity patterns were determined using the double-coupled assay, varying MgATP at several fixed concentrations of F6P. Inhibition patterns were also determined using the double-coupled assay, fixing F6P equal to its K_m value and varying MgATP at several different concentrations of inhibitor. The individual K_{F6P} and V values, which are used in the isotope partitioning calculations, were determined using the adolase/triose phosphate isomerase/α-glycerolphosphate dehydrogenase coupled assay, fixing one substrate at a saturating concentration and varying the other substrate. To avoid activation of PFK by $(NH_4)_2SO_4$, all coupling enzyme stock solutions were prepared either by desalting an ammonium sulfate suspension of the enzyme using a Centricon-30 centrifuge/filter apparatus or by dissolving an $(NH_4)_2SO_4$-free lyophilized powder of the enzyme.

Mg^{2+}−Chelate Correction. All previous *A. suum* PFK initial velocity experiments were carried out at an arbitrary high $[Mg^{2+}]$ concentration so that all ATP would be present as MgATP, the true substrate for PFK. However, in studying the effect of the Mg^{2+} ion on PFK activity, it was necessary to correct for the presence of all Mg−ligand complexes present in a reaction mixture. The concentration of substrates, effectors, and inhibitors was corrected for the concentration of any metal−ligand complex at a given $[Mg^{2+}]_{free}$ concentration using eq 1

$$[L]_t = [L]_{free} + \frac{[L]_{free}[Mg^{2+}]_{free}}{K_{ML}} \quad (1)$$

where $[L]_t$ is the total ligand concentration in the reaction mixture, $[L]_{free}$ is the desired concentration of free Mg^{2+}, and K_{ML} is the equilibrium constant for dissociation of the Mg−ligand complex. The total concentration of Mg^{2+} ions to be added to a reaction mixture containing i ligands was calculated according to eq 2

$$[Mg^{2+}]_t = [Mg^{2+}]_{free} + \sum \frac{[Mg^{2+}]_{free}[L_i]_{free}}{K_{ML_i}} \quad (2)$$

where $[Mg^{2+}]_{free}$ is the total concentration of Mg^{2+} to be added to the reaction mixture, $[L_i]_{free}$ is the desired concentration of the ith ligand, and K_{ML_i} is the equilibrium constant for dissociation of the chelate complex between Mg^{2+} and the ith ligand. Results at "low" Mg^{2+} are those obtained at the fixed free Mg^{2+} concentration of 0.1 mM, while experiments at "high" Mg^{2+} are those obtained at 5 mM free Mg^{2+} concentration.

A dissociation constant of 15 μM was used for the MgATP complex (*10*), while a dissociation constant of 25 mM was used for the MgF6P complex (*11*). At low Mg^{2+}, about 15% of the ATP is uncomplexed. It has been shown previously that uncomplexed Mg^{2+} only binds to the allosteric inhibitory site, which has very low affinity for the nucleotide in dPFK (*3*).

Isotope Partitioning Studies. Isotope partitioning experiments were performed at 30 °C according to the method of Rose (*12*) at 5 mM Mg^{2+} and 0.1 mM Mg^{2+} for the dPFK:MgATP* complex. Experiments were carried out in the absence and presence of $F26P_2$. The method for experiments at high Mg^{2+} are described first, followed by the method for experiments at low Mg^{2+}.

For the high Mg^{2+} dPFK:MgATP* experiment in the absence of $F26P_2$, the pulse consisted of 130 μM dPFK (on the basis of a MW of 9000/subunit) and 0.24 mM MgATP*

(9000 cpm/nmol) in a total volume of 50 μL. The chase consisted of 100 mM imidazole-HCl (pH 6.8), 2.0 mM MgATP, and 0.5, 1.0, 4.2, or 10.0 mM F6P in a total volume of 5 mL. Using a K_D value of 2.0 μM for the dPFK:MgATP* complex at 8 mM Mg^{2+}, [dPFK:MgATP*]$_0$ is 129 μM. For experiments in the presence of saturating $F26P_2$, the pulse consisted of 60 μM dPFK, 0.24 mM MgATP* (9000 cpm/nmol), and 0.2 mM $F26P_2$ in a total volume of 50 μL, and the chase consisted of 100 mM imidazole-HCl (pH 6.8), 2.0 mM MgATP, and 0.2, 0.5, 1.0, or 10.0 mM F6P plus 0.2 mM $F26P_2$ in a total volume of 5 mL. Using a K_D value of 2.3 μM for the dPFK:MgATP* complex at 8 mM Mg^{2+}, [dPFK:MgATP*]$_0$ is 59 μM.

For the low Mg^{2+} dPFK:MgATP* experiments in the absence or presence of $F26P_2$, the pulse consisted of 0.1 mM dPFK and 0.2 mM MgATP* (10 000 cpm/nmol), plus and minus 0.2 mM $F26P_2$ in a total volume of 50 μL. The chase consisted of 50 mM imidazole-HCl (pH 6.8), 2.0 mM MgATP, and 0.25. 0.5, 1.0, or 20 mM F6P in a total volume of 5 mL. Using a K_D value of 30 μM for the dPFK:MgATP complex at 0.1 mM Mg^{2+} in the absence of $F26P_2$, [dPFK:MgATP]$_0$ is 80 μM. Using a K_D value of 38 μM in the presence of $F26P_2$, [dPFK:MgATP]$_0$ is 76 μM.

To allow a reliable comparison of the isotope partitioning data at 0.1 and 5 mM Mg^{2+}, experiments at high Mg^{2+} were repeated using the same enzyme stock as that used in the low Mg^{2+} experiments. The Mg^{2+} concentration was fixed at 5 mM, correcting for the presence of MgATP and MgF6P as discussed above. The pulse consisted of 0.1 mM dPFK and 0.2 mM MgATP* (10 000 cpm/nmol) plus and minus 0.2 mM $F26P_2$ in a total volume of 50 μL. The chase consisted of 50 mM imidazole-HCl (pH 6.8), 2.0 mM MgATP, and 0.5 or 10.0 mM F6P in a total volume of 5 mL. Assuming a K_D value of 2 μM for the dPFK:MgATP complex at high Mg^{2+}, [dPFK:MgATP]$_0$ is 98 μM.

For all isotope partitioning experiments, the pulse was added to the rapidly stirring chase solution, and the reaction was quenched after 3 s by adding 200 mM ethylenediamine tetraacetate (EDTA). A 1 mL aliquot of the quenched reaction mix was then injected onto a Whatman Partisil 10-SAX column, with 250 mM phosphate as the running buffer, a gradient from 0 to 1.5 M KCl, and a flow rate of 2 mL/min. Fractions of 2 mL were collected, and the amounts of MgATP* were determined by scintillation counting. For each experiment, two controls were carried out. The first control was a measure of trapping at 0 substrate in the chase, thus accounting for any ATPase reaction in the pulse solution. This control was necessary because P_i and FBP coelute from the anion-exchange column under these conditions. The second control was carried out for each concentration of varied substrate in the chase solution. The enzyme alone was added to the chase solution containing the same amount of radio-labeled substrate present in the pulse, thus accounting for any steady-state production of radio-labeled product in the pulse/chase mixture. All data points and controls were the average of duplicate experiments.

Data Processing. Steady-state kinetic data were fitted using the appropriate rate equations and computer programs developed by Cleland (*13*). Equation 3 was used for substrate saturation curves. Equation 4 was used for initial velocity patterns in the absence of inhibitors. Equation 5 was used for noncompetitive inhibition patterns, where one substrate was fixed and the other substrate was varied at several different concentrations of inhibitor. Equation 6 was used for the initial velocity pattern at varied Mg^{2+} and MgATP with F6P fixed. Isotope partitioning data were fitted using eq 3 with P^* and P^*_{max} substituted for v and V and K'_a (K_m for trapping) substituted for K_a.

$$v = \frac{VA}{K_a + A} \tag{3}$$

$$v = \frac{VAB}{K_{ia}K_b + K_aB + K_bA + AB} \tag{4}$$

$$v = \frac{VA}{K_a\left(1 + \frac{I}{K_{is}}\right) + A\left(1 + \frac{I}{K_{ii}}\right)} \tag{5}$$

$$v = \frac{VAB}{K_{ia}K_b + K_bA + AB} \tag{6}$$

In eqs 3−6, v and V are initial and maximum velocities, A, B, and I are reactant and inhibitor concentrations, K_a and K_b are Michaelis constants for A and B, K_{ia}, K_{is}, and K_{ii} are inhibition constants for A, slope, and intercept, respectively.

RESULTS

The initial rate of the *A. suum* PFK reaction is faster at high (8.0 mM) than at low (1.0 mM) Mg^{2+}. At 1 mM Mg^{2+}, sufficient metal ion is available to completely convert all of the ATP to its metal−chelate complex. The observation suggests that Mg^{2+} may play a role in the reaction distinct from that of forming the MgATP chelate complex. The fact that the $[Mg^{2+}]_{free}$ concentration might affect the catalytic activity of PFK is not unprecedented. Many enzymes catalyzing phosphoryl transfer reactions have been shown to require more than a single divalent metal ion for catalysis, including the catalytic subunit of cyclic AMP-dependent protein kinase (*14*), choline kinase (*15*), pyrophosphatase (*16*, *17*), sodium/potassium ATPase (*18*), and pyrophosphate-dependent PFK (*19*). To determine whether a second, catalytically important metal ion contributes to the *A. suum* PFK reaction, initial rate measurements were carried out as a function of the Mg_{free} concentration. All experiments were carried out with the dPFK at pH 6.8. dPFK is the diethylpyrocarbonate-modified enzyme desensitized to allosteric inhibition by ATP (*2*). Although subtle differences may exist between the nPFK (native enzyme) at pH 8.0, where the enzyme is noncooperative, and the dPFK at pH 6.8, the basic mechanisms are the same for both enzymes (*2*, *3*).

Initial Velocity Studies at Varied Mg^{2+}. To determine whether the steady-state kinetic parameters, V, K_{F6P}, and K_{MgATP}, are affected by the concentration of Mg^{2+}, initial velocity experiments were carried out. The initial rate of the dPFK reaction was measured with F6P and ATP concentrations fixed at their respective K_m values while varying the total Mg^{2+} concentration (Figure 1). The Mg^{2+} dependence of the reaction velocity under these conditions is biphasic, giving apparent activation constants of approximately 15 and 200 μM. Mg^{2+} appears to have a slight inhibitory effect at concentrations above 5 mM.

To determine the details of the Mg^{2+} activation, initial velocity patterns were obtained varying MgATP at several fixed levels of F6P, and this pattern was then repeated at

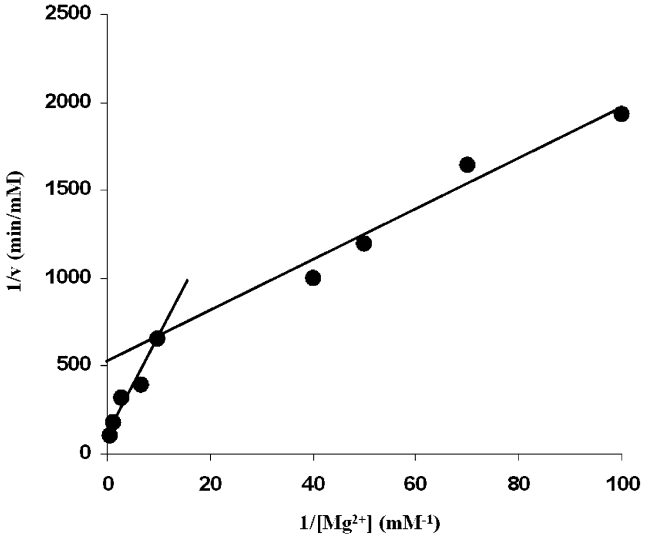

FIGURE 1: Activation of dPFK by Mg^{2+} in the absence of $F26P_2$. The concentrations of ATP and F6P were fixed around their respective K_m values (assuming that ATP is present as MgATP), while the total Mg^{2+} concentration was varied without correction for the metal−substrate complexes. The two lines are based on linear regression analysis of the data at the lowest 5 points and the highest 5 points to illustrate the biphasic nature of the plot. Initial rates were measured at pH 6.8, 100 mM imidazole-HCl, and 25 °C.

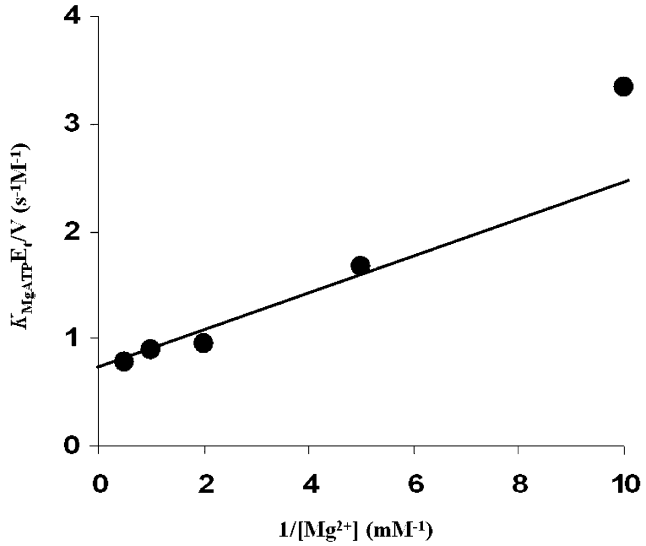

FIGURE 2: K_{act} plot for Mg^{2+} activation of dPFK (pH 6.8). The reciprocal of the V/K_{MgATP} values obtained from initial velocity patterns at different Mg^{2+} concentrations are plotted versus the reciprocal of the Mg^{2+} concentration. The data are fitted to eq 3, where v and V are substituted by V/K_{MgATP} and $(V/K_{MgATP})_{max}$, A is the Mg^{2+} concentration, and K_a is K_{act} for Mg^{2+}.

several fixed concentrations of Mg^{2+} (data not shown). Kinetic parameters obtained at low and high Mg^{2+} are summarized in Table 1. The pattern obtained at a low Mg^{2+} concentration intersects to the left of the ordinate, while the pattern at high Mg^{2+} exhibits near parallel lines. The parallel pattern is likely due to a low K_i/K_m ratio for MgATP, and the qualitative difference between the two patterns is likely caused by Mg^{2+} affecting this ratio. For patterns obtained at 0.1, 0.2, 0.5, 1.0, and 2.0 mM Mg^{2+}, V/K_{F6P} is independent of the Mg^{2+} concentration. The value of V/K_{MgATP} is increased with an increasing Mg^{2+} concentration, and a double-reciprocal plot of V/K_{MgATP} versus Mg^{2+} is shown in Figure 2. A fit of the data using eq 3 gives an activation constant (K_{act}) for Mg^{2+} of 0.31 ± 0.07 mM. The lowest concentration point deviates from the fitted line as a result of experimental error.

Because there is no change in K_{F6P} as the Mg^{2+} concentration is changed, F6P was maintained saturating (20 mM) and an initial velocity pattern was obtained varying the Mg^{2+} concentration at several different fixed concentrations of MgATP (Figure 3). The initial velocity pattern intersects on the ordinate, indicating an equilibrium-ordered addition of Mg^{2+} before MgATP. A fit of the data using eq 4 gives a K_{MgATP} value of 19 ± 2 μM and a $K_{iMg^{2+}}$ value of 0.47 ± 0.08 mM. The Mg^{2+}-independent value of V/E_t from Figure 3 is 38 ± 2 s^{-1} (Table 1).

Repeating the above experiments in the presence of saturating $F26P_2$, an allosteric activator of PFK, gives a V/E_t value of 36 ± 3 s^{-1} (Table 1), which is, within error, equal to the value obtained in the absence of $F26P_2$. The corresponding K_{F6P} values in the absence and presence of $F26P_2$ are 0.49 ± 0.07 and 0.15 ± 0.01 mM, respectively, and the change in K_{F6P} is independent of the Mg^{2+} concentration (Table 1).

Table 1: Summary of the Data from Isotope Partitioning for dPFK:MgATP* at Low and High[a] Mg^{2+}

	5 mM Mg^{2+}		0.1 mM Mg^{2+}	
	−$F26P_2$	+$F26P_2$	−$F26P_2$	+$F26P_2$
V/E_t (s^{-1})	38 ± 2	36 ± 3	38 ± 2	36 ± 3
K_{F6P} (mM)[b]	1.2 ± 0.1	0.13 ± 0.01	0.49 ± 0.07	0.15 ± 0.01
K_{iMgATP} (μM)[c]	2.0 ± 0.5	2.3 ± 0.7	30 ± 15	38 ± 10
P^*_{max} (μM)	93[a] (95%)	67 (68%)	16 ± 1 (20 ± 1%)	16 ± 1 (20 ± 1%)[a]
K'_{F6P} (mM)	0.76	0.15	0.66 ± 0.05	0.08 ± 0.01
$[E:A]_0/P^*_{max}$	1.05 ± 0.10	1.147 ± 0.12	5.0 ± 0.5	5.0 ± 0.5
k_{off} (s^{-1})	25 ± 7	44 ± 9 to 64 ± 12	48 ± 12 to 240 ± 60	19 ± 5 to 100 ± 25
k_7/k'_5		0.50	4.0 ± 0.3	4.0 ± 0.3
k_7 (s^{-1})		18 ± 2	145 ± 5	145 ± 5
k_{on} (M^{-1} s^{-1})	(1.3 ± 0.5) × 10^7	(1.9 ± 0.8) × 10^7 to (2.8 ± 1.4) × 10^8	(1.6 ± 0.9) × 10^6 to (8.1 ± 3.9) × 10^6	(6.3 ± 3.2) × 10^5 to (3.2 ± 1.4) × 10^6

[a] Mg^{2+} (5 mM) data were obtained as a repeat of the high Mg^{2+} data for dPFK (*7*) using the same enzyme preparation that was used in experiments at 0.1 mM Mg^{2+}. This was to ensure that apparent Mg^{2+} effects on isotope partitioning parameters were not caused by changes in the enzyme preparations. Only two points were measured for each of the ±$F26P_2$ experiments; therefore, no error estimates are given. [b] All K_{F6P} values were determined using the single aldolase/trisephosphate isomerase/α-glycerolphosphate dehydrogenase coupled assay with coupling enzyme solutions made fresh from lyophilized powder to avoid the affects of $(NH_4)_2SO_4$ on K_{F6P}. [c] For data at 5 mM Mg^{2+}, K_{iMgATP} was calculated from the CD studies; for data at 0.1 mM Mg^{2+}, K_{iMgATP} was obtained as an estimate from a computer fit of eq 4 to the initial velocity data.

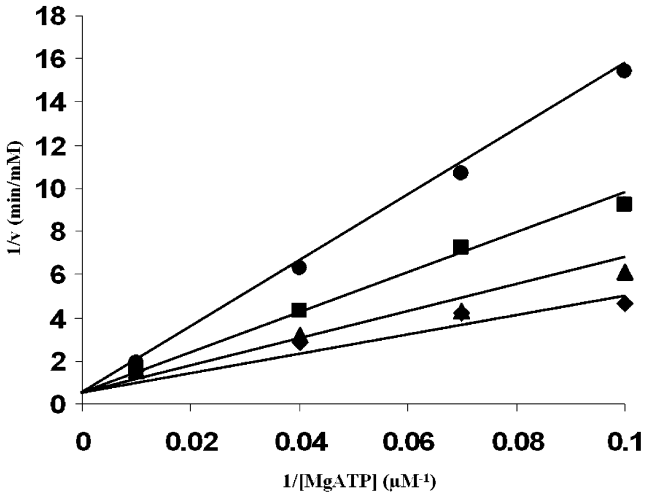

FIGURE 3: Initial velocity pattern varying MgATP and Mg^{2+} with F6P fixed at saturation. The lines are the best fit of the data to eq 6, while the points are experimental values. The symbols represent 0.1 mM Mg^{2+} (●), 0.5 mM Mg^{2+} (■), 1.0 mM Mg^{2+} (▲), and 2.0 mM Mg^{2+} (◆).

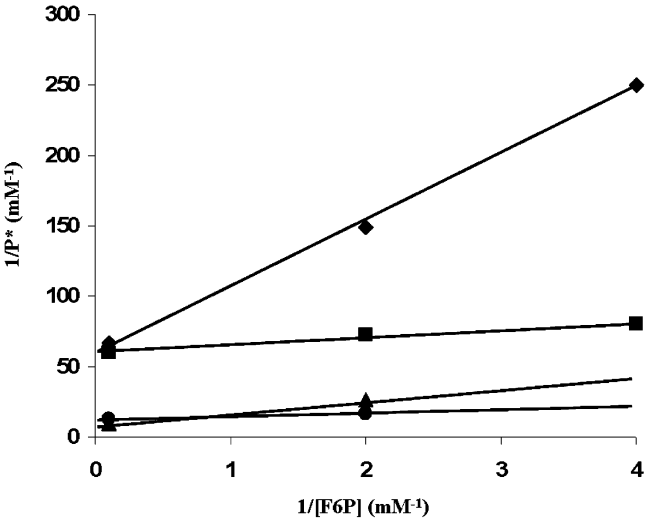

FIGURE 4: Isotope trapping of the dPFK:MgATP* complex at 0.1 mM (◆ and ■) and 5.0 mM (▲ and ●) Mg^{2+} in the absence (◆ and ▲) and presence (■ and ●) of 0.2 mM $F26P_2$. The amount of [1-^{32}P]FBP formed at different concentrations of F6P in the chase solution was determined as described in the text. The lines are the best fit of the data using eq 3, while the points are experimental values.

Isotope Partitioning of dPFK:MgATP in the Absence or Presence of F26P$_2$.* To obtain further information on the mechanism of Mg^{2+} activation, isotope partitioning experiments were carried out at low and high Mg^{2+} concentrations in the absence and presence of $F26P_2$. The partitioning of the dPFK:MgATP* complex at 0.1 mM Mg^{2+} in the presence or absence of $F26P_2$ is shown in Figure 4. In both cases, a P^*_{max} of 16 ± 1 μM is obtained, representing 20% of the MgATP bound in the initial binary complex, using dissociation constants of 30 ± 15 and 38 ± 10 μM for the dPFK:MgATP complex in the absence and presence of $F26P_2$, respectively (Table 1). In the absence of $F26P_2$, a K'_{F6P} value of 0.66 ± 0.05 mM is obtained, while in the presence of $F26P_2$, the value decreases by about 8-fold to 0.08 ± 0.01 mM.

Partitioning the dPFK:MgATP* complex at 5 mM Mg^{2+} in the presence or absence of $F26P_2$ is also shown in Figure 4. P^*_{max} values of 93 and 67 μM in the absence and presence of $F26P_2$, respectively, represent 95 and 68% of the MgATP* bound in the initial binary complex. The corresponding K'_{F6P} values are 0.76 and 0.15 mM, respectively. Data are summarized in Table 1.

Arabinose 5-Phosphate Inhibition. The arabinose 5-phosphate (Ara5P) versus MgATP inhibition patterns for dPFK at 0.1 mM Mg^{2+} were obtained in the absence and presence of $F26P_2$ (data not shown). Data adhere to noncompetitive inhibition for both inhibition patterns. In the absence of $F26P_2$, a fit of the data using eq 5 gives a K_{MgATP} of 33 ± 2 μM, a K_{is} of 23 ± 6 μM, and a K_{ii} of 5.0 ± 0.3 mM. In the presence of $F26P_2$, a fit of the data using eq 6 yields a K_{MgATP} of 34 ± 2 μM, a K_{is} of 7 ± 1 mM, and a K_{ii} of 8 ± 1 mM.

DISCUSSION

For concentrations of ATP less than 0.5 mM, a total Mg^{2+} concentration of 1 mM ensures that essentially 100% of the ATP in a reaction mixture is present as MgATP. However, the rate of the PFK reaction is faster at 8 mM than at 1 mM total Mg^{2+}, a phenomenon that cannot be explained simply by a difference in the concentration of the substrate MgATP at the two levels of Mg^{2+}. The latter finding suggests an activating effect of Mg^{2+} on the *A. suum* PFK and led to the experiments at varied Mg^{2+} described above.

Initial Velocity Studies at Varied Mg^{2+}. The double-reciprocal plot shown in Figure 1 shows a biphasic saturation curve for total Mg^{2+}, giving apparent activation constants of approximately 15 and 200 μM. Because the total Mg^{2+} concentration in these assays was not corrected for the formation of the MgATP complex, the lower constant of 15 μM likely represents the titration of ATP to form the substrate MgATP. The value of 15 μM is in excellent agreement with the dissociation constant for the MgATP complex reported previously (*3*, *7*, *11*). The 200 μM activation constant likely represents binding of free Mg^{2+} to some form of the enzyme.

Activation of the dPFK by Mg^{2+} is more easily seen in the initial velocity patterns at low and high Mg^{2+} (Table 1). A qualitative change in the initial velocity pattern from intersecting at low Mg^{2+} to near parallel at high Mg^{2+} suggests a decrease in the K_d/K_m ratio for MgATP (data not shown). In agreement, K_{iMgATP} decreases about 15-fold as the Mg^{2+} concentration increases from 0.1 to 5 mM (Table 1), while only a 3−4-fold decrease in K_{MgATP} is observed over the same range; V and K_{F6P} do not change appreciably. A K_{act} for Mg^{2+} of 0.31 ± 0.07 mM is estimated from the Mg dependence of V/K_{MgATP} (Figure 2). Thus, activation is observed only under conditions where MgATP is limiting. An initial velocity pattern obtained with saturating F6P, varying the concentration of MgATP at different fixed concentrations of Mg^{2+} intersects on the ordinate indicative of an equilibrium-ordered addition of Mg^{2+} prior to MgATP. A K_{act} for Mg^{2+} obtained from the data in Figure 3 is 0.47 ± 0.08 mM, in good agreement with the apparent activation constants obtained from the data in Figures 1 and 2. In addition, values for K_{MgATP} (19 μM) and $V/K_{MgATP}E_t$ (1.9×10^6 M^{-1} s^{-1}) are both in excellent agreement with values reported by Payne et al. (*20*). Of interest, $F26P_2$ has no effect on the K_{act} for Mg^{2+} or K_{MgATP} (Table 1; *1*).

Inhibition patterns obtained with Ara5P are noncompetitive at 0.1 mM Mg^{2+}, indicating that the F6P analogue is able to bind to the enzyme both before and after MgATP in the absence or presence of $F26P_2$. These data are consistent with the noncompetitive inhibition pattern obtained for dPFK at 8 mM Mg^{2+} in the presence of $F26P_2$ (*1*). Thus, it appears that the absence of the second Mg^{2+} has the same effect as high Mg^{2+} in the presence of $F26P_2$, i.e., an increase in the off rate for MgATP from the central complex.

Mg^{2+} Dependence of Partitioning of the E:MgATP Complex. At 0.1 mM Mg^{2+}, a P^*_{max} of 16 μM is measured, indicating about 20% trapping of the E:MgATP* complex at infinite F6P. This can be compared to a value of 93 μM at 5 mM Mg^{2+}, indicative of about 95% trapping. The amount of trapping is corrected for a decrease in the specific activity of dPFK compared to the nPFK from which it was prepared as a result of the inactivation of some of the enzyme during its preparation. The dPFK is prepared by diethylpyrocarbonate (DEPC) modification of the ATP allosteric site, with the enzyme active site protected from modification by bound F6P (*3*). The inactivation is expected because the concentration of F6P cannot be maintained high enough to give complete saturation at the active site. When inactive dPFK is taken into account, all of the E:MgATP* complex, within error, is trapped at high Mg^{2+}, consistent with an ordered kinetic mechanism with F6P binding after MgATP. Data are in agreement with previous studies obtained using 8 mM Mg^{2+} (*1*, *6*). The partial trapping at low Mg^{2+} indicates that MgATP is able to dissociate from the ternary complex.

At high Mg^{2+}, 100%, within error, of the estimated E:MgATP* complex was trapped as discussed above, consistent with an ordered addition of MgATP before F6P, in agreement with previously published isotope partitioning (*1*) and initial velocity data (*6*). However, even 100% trapping of the E:MgATP complex does not rule out the possibility of a random mechanism but only suggests that catalysis is much faster than MgATP dissociation. Indeed, the fact that F6P alone protects the active site against DEPC modification suggests that a minor pathway in which F6P binds to the enzyme prior to MgATP may exist. However, the high K_D (50−60 mM) for the E:F6P complex estimated from the F6P protection against DEPC modification (*3*) compared to the low K_D (2 μM) for the E:MgATP complex and the rate constants for dissociation of E:MgATP:F6P gives an essentially ordered mechanism. Formally, the mechanism can be described as random with a high degree of synergism of substrate binding.

The K'_{F6P} value of 0.76 ± 0.15 mM obtained at high Mg^{2+} allows estimation of the off rate of MgATP from the binary complex using eq 7 (*13*)

$$\left(\frac{K'_{F6P}}{K_{F6P}}\right)\left(\frac{V}{E_t}\right) < k_{off} < \left(\frac{K'_{F6P}}{K_{F6P}}\right)\left(\frac{V}{E_t}\right)\left(\frac{[E:MgATP^*]_0}{P^*_{max}}\right) \quad (7)$$

From Table 1, at 5 mM Mg^{2+}, values for V/E_t, K_{F6P}, $[E:MgATP^*]_0/P^*_{max}$ are 38 ± 2, 1.2 ± 0.1, and 1.05 ± 0.10, respectively. Assuming 100% trapping, the estimated k_{off} for MgATP from the E:MgATP complex is about 25 ± 5 s^{-1} within a factor of 2 of the value of 42 s^{-1} obtained at 8 mM Mg^{2+} (*1*). Using the dissociation constant value of 2 μM, K_{iMgATP} in Table 1, an on rate for MgATP binding to the enzyme is about 10^7 M^{-1} s^{-1}, which is about 10−100-fold lower than the diffusion-limited rate of combination of a small molecule and a macromolecule (*20*). The difference in the estimated on rate and the known diffusion rate is in agreement with previous studies, which suggest an isomerization of the E:MgATP complex (*1*).

Scheme 1: Kinetic Scheme for Partitioning of the E:MgATP* Complex in the *A. suum* PFK Reaction

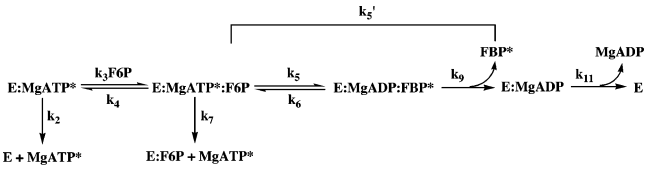

At 0.1 mM Mg^{2+}, where less than 100% trapping is estimated, the partition ratio k_7/k_5' (Scheme 1) can be calculated using eq 8

$$\frac{k_7}{k'_5} = \left(\frac{[E:MgATP^*]_0}{P^*_{max}}\right) - 1 \quad (8)$$

In Scheme 1, k_5' is the net rate constant for all steps involved in converting the E:MgATP:F6P complex to products and the release of the first product. Release of MgADP is rapid, as demonstrated by initial rate studies, and thus, $V/E_t \sim k_5'$ (*6*). The partition ratio is 0 when 100% trapping occurs; $k_7 \ll k_5'$, as found at 5 mM Mg^{2+}. The 20% trapping at low Mg^{2+} gives a partition ratio (k_7/k_5') of 4 (Table 1). Because the rate at the saturating reactant concentration is independent of Mg^{2+}, the increase in the partition ratio observed at low Mg^{2+} (Table 1) likely results from an increase in k_7, the off-rate constant for MgATP from the central E:MgATP:F6P complex. The second Mg^{2+} thus functions by increasing the affinity for MgATP in the central complex. The increase in the off rate of MgATP from the ternary complex at low Mg^{2+} is consistent with the 15-fold increase in the K_D (compared to high Mg^{2+}) for the E:MgATP binary complex. A k_5' value of 36 ± 3 s^{-1} at low Mg^{2+} gives a value of 144 ± 16 s^{-1} for k_7 using the value of 4.0 ± 0.3 for k_7/k_5'. It should be pointed out that previous attempts to trap the dPFK:^{14}C-F6P complex failed, suggesting an ordered mechanism (*1*). The absence of F6P trapping does not, however, rule out a random mechanism with respect to MgATP and F6P but only suggests that either the E:F6P complex does not form (or has a K_D much larger than the concentration of F6P used in the pulse solution), or that the off rate for F6P is much faster than catalysis. Such a "leaky" ternary complex is consistent with the random kinetic mechanism observed previously for dPFK in the presence of $F26P_2$ (see below; *1*).

Isotope trapping gives a K'_{F6P} of 0.66 ± 0.05 mM at 0.1 mM Mg^{2+}, similar to the value of 0.85 ± 0.15 mM at high Mg^{2+} (Table 1). Using eq 7 and the values measured in Table 1, a range from 48 ± 12 to 240 ± 60 s^{-1} is calculated for k_{off}. Given a dissociation constant of 30 μM for the E:MgATP complex, an on rate of about (2−8) × 10^6 M^{-1} s^{-1} is calculated, which is at least 100-fold slower than the estimated diffusion rate. In addition, the 15-fold increase in K_{iMgATP} at low compared to high Mg^{2+} results from a 2−9-fold increase in the off-rate constant for MgATP from the binary complex and a 1.5−6-fold decrease in the on-rate constant for MgATP to form E:MgATP.

Effects of F26P$_2$ on the PFK-Catalyzed Reaction. In the presence of F26P$_2$, a value of k_7/k_5' can be calculated at high and low Mg^{2+} because less than 100% trapping of E:MgATP* was observed in both cases. As shown in Table 1, values of 0.5 and 4 are obtained for the ratio at high and low Mg^{2+}. The value estimated at low Mg^{2+} is not affected by F26P$_2$, while a finite value of k_7/k_5' is observed at high Mg^{2+}. The value of k_7 at high Mg^{2+} in the absence of F26P$_2$ is essentially 0 (100% trapping), while in the presence of F26P$_2$, it is finite but 8-fold lower than the F26P$_2$-independent value of k_7 obtained at low Mg^{2+}. In the presence of F26P$_2$, the K_{F6P} value decreases to 0.08 ± 0.1 mM, which is about 3-fold less than the value of 0.26 ± 0.07 mM obtained for K'_{F6P} at high Mg^{2+}. The K'_{F6P} value obtained at low Mg^{2+} in the presence of F26P$_2$ is about 8-fold lower than that obtained in the absence of F26P$_2$. Using eq 7, the value for k_{off} for MgATP from E:MgATP in the presence of F26P$_2$ is in the range from 19 ± 5 to 100 ± 25 s^{-1} at low Mg^{2+} and from 44 ± 9 to 64 ± 12 s^{-1} at high Mg^{2+}. Using a dissociation constant of 30 μM for the E:MgATP complex in the presence of F26P$_2$, the on rate is on the order of 10^6 M^{-1} s^{-1}, similar to values estimated above in the absence of F26P$_2$. Data at low Mg^{2+} are, within error, equal in the absence and presence of F26P$_2$.

The main effect of F26P$_2$ on the PFK reaction is to increase the affinity for F6P (*7*, *21*). Payne et al. have suggested that the binding of F26P$_2$ to its allosteric site decreases the off rate for F6P. Isotope partitioning data (*1*; present study) are consistent with the previously proposed role for F26P$_2$. At high Mg^{2+}, the leakiness of the ternary complex is observed with respect to MgATP release from the E:MgATP:F6P ternary complex as a result of an increase in the affinity for F6P. At low Mg^{2+}, no effect of F26P$_2$ is observed on the off rate for MgATP from either binary or ternary complexes. The combined effect of Mg^{2+} and F26P$_2$ is to increase the concentration of the Michaelis complex and thus the rate of the overall reaction.

Effects of Mg^{2+} on the PFK-Catalyzed Reaction. Initial velocity studies at varied Mg^{2+} indicate an activating effect of the metal ion, giving an increase in the apparent affinity of PFK for MgATP with an increase in Mg^{2+}. As with the activator F26P$_2$, the parameter V is not affected by Mg^{2+}. Assuming that the rate of the forward reaction is not limited by the product release so that V represents the catalytic steps, Mg^{2+} must activate by decreasing the off rate for MgATP. Although the specific role of Mg^{2+} in decreasing the off rate for MgATP is uncertain, it is likely that the metal ion acts at the active site and not as an allosteric site. A number of enzymes catalyzing phosphoryl transfer reactions have been identified that indicate that Mg^{2+} is an active-site effector (*16*−*19*, *22*). The role of a second Mg^{2+} in decreasing the off rate for MgATP could simply be structural, maintaining the proper enzyme conformation, or chemical, neutralizing the negative charge(s) on MgATP. The freely dissociable Mg^{2+} has an effect on the affinity of PFK for MgATP and may have an effect on the reaction chemistry, acting as a Lewis acid to polarize the γ phosphoryl and neutralizing the negative charge on the α and/or γ phosphate of MgATP. Overall, this would facilitate nucleophilic attack by the hydroxyl group of F6P.

If Mg^{2+} were an essential activator of *A. suum* PFK, then no activity should occur in its absence. The reaction rate measured in the absence of any added Mg^{2+} is finite (data not shown), being 30% of the rate measured at 10 μM of added Mg^{2+}. However, the addition of micromolar amounts of EDTA to the reaction mixture eliminates the activity. The small residual activity likely results from contaminating Mg^{2+} (or other divalent metal ions) in the reaction buffer, because decreasing the concentration of the imidazole reaction buffer from 100 to 20 mM causes a decrease in the activity at 0 added Mg^{2+}. Bertagnolli and Cook (*19*) used atomic absorption analysis to show that a background level of as much as 5 μM Mg^{2+} may be present in a reaction mixture similar to the one used in the above-mentioned assays, with most or all of the contaminating Mg^{2+} coming from the buffer.

Although Mg^{2+} activation of the PFK activity has been treated as occurring from the binding of a second metal in addition to that bound in the MgATP metal−chelate complex, the actual stoichiometry of Mg^{2+} binding is not known. Indeed, multiple metal ions may be involved in activating the enzyme. Knight et al. (*16*) showed through nuclear magnetic resonance and electron paramagnetic resonance experiments on the yeast inorganic pyrophosphatase that two divalent cations are necessary at the active site for catalysis to occur in addition to the one divalent cation involved in forming the metal−PP_i complex. Also unknown for the *A. suum* PFK is the physiological significance of Mg^{2+} as an effector of the enzyme. However, the estimated K_{act} for Mg^{2+} (0.4 mM) is within the range of the estimated physiological concentration of 0.5 mM Mg^{2+} in *A. suum* muscle tissue (*23*), suggesting a likely importance. Further studies are necessary to elucidate the stoichiometry and chemical role of metal ion binding to the *A. suum* PFK.

REFERENCES

1. Gibson, G. E., Harris, B. G., and Cook, P. F. (1996) Isotope Partitioning with *Ascaris suum* Phosphofructokinase Is Consistent with an Ordered Kinetic Mechanism, *Biochemistry 35*, 5451−5457.
2. Rao, G. S. J., Cook, P. F., and Harris, B. G. (1991) Effector-Induced Conformational Transitions in *Ascaris suum* Phosphofructokinase, *J. Biol. Chem. 266*, 8884−8890.
3. Rao, G. S. J., Wariso, B. A., Cook, P. F., Hofer, H. W., and Harris, B. G. (1987) Reaction of *Ascaris suum* Phosphofructokinase with Diethylpyrocarbonate: Inactivation and Desensitization to Allosteric Modulation, *J. Biol. Chem. 262*, 14068−14073.
4. Rao, G. S. J., Cook, P. F., and Harris, B. G. (1991) Modification of the ATP Inhibitory Site of the *Ascaris suum* Phosphofructokinase Results in the Stabilization of an Inactive T State, *Biochemistry 30*, 9998−10004.
5. Rao, G. S. J., Schnackerz, K. D., Harris, B. G., and Cook, P. F. (1995) A pH-Dependent Allosteric Transition in *Ascaris suum* Phosphofructokinase Distinct from That Observed with Fructose 2,6-Bisphosphate, *Arch. Biochem. Biophys. 322*, 410−416.
6. Rao, G. S. J., Harris, B. G., and Cook, P. F. (1987) Kinetic Mechanism of *Ascaris suum* Phosphofructokinase Desensitized to Allosteric Modulation by Diethylpyrocarbonate Modification, *J. Biol. Chem. 252*, 14074−14079.
7. Payne, M. A., Rao, G. S. J., Harris, B. G., and Cook, P. F. (1991) Fructose 2,6-Bisphosphate and AMP Increase the Affinity of the *Ascaris suum* Phosphofructokinase for Fructose 6-Phosphate in a Process Separate from the Relief of ATP Inhibition, *J. Biol. Chem. 266*, 8891−8896.
8. Starling, J. A., Allen, B. L., Kaeini, M. R., Payne, D. M., Blytt, H. J., Hofer, H. W., and Harris, B. G. (1982) Phosphofructokinase from *Ascaric suum*. Purificaton and Properties, *J. Biol. Chem. 257*, 3795−3800.
9. Bradford, M. M. (1976) A Rapid and Sensitive Method for the Quantitation of Microgram Quantities of Protein Utilizing the Principle of Protein−Dye Binding, *Anal. Biochem. 72*, 248−254.

10. Dawson, R. M. C., Elliott, D. C., Elliott, W. H., and Jones, K. M. (1986) *Data for Biochemical Research*, 3rd ed., Oxford University Press, New York.
11. Martell, A. E., and Smith, R. M. (1982) *Critical Stability Constants*, Vol. 5, Plenum Press, New York.
12. Rose, I. A. (1980) The Isotope Trapping Method: Desorption Rate of Produtive E.S. Complexes, *Methods Enzymol. 64*, 47−59.
13. Cleland, W. W. (1979) Statistical Analysis of Enzyme Kinetic Data, *Methods Enzymol. 63*, 103−109.
14. Cook, P. F., Neville, M. E., Jr., Vrana, K. F., Hartl, F. T., and Roskoski, R., Jr. (1982) Adenosine Cyclic 3′,5′-Monophosphate Dependent Protein Kinase: Kinetic Mechanism for the Bovine Skeletal Muscle Catalytic Subunit, *Biochemistry 21*, 5794−5799.
15. Reinhardt, R. R., Wecker, L., and Cook, P. F. (1984) Kinetic Mechanism of Choline Kinase from Rat Striata, *J. Biol. Chem. 259*, 7446−7452.
16. Knight, W. B., Dunaway-Mariano, D., Ransom, S. C., and Villafranca, J. J. (1984) Investigations of the Metal Ion-Binding Sites of Yeast Inorganic Pyrophosphatase, *J. Biol. Chem. 259*, 2886−2895.
17. Sosa, A., Ordaz, H., Romero, I., and Celis, H. (1992) Mg^{2+} is an Essential Activator of Hydrolytic Activity of Membrane-Bound Pyrophosphatase of *Rhodospirillum rubrum*, *Biochem. J. 283*, 561−566.
18. Campos, M., and Beague, L. (1992) Effects of Magnesium and ATP on Pre-Steady-State Phosphorylation Kinetics of the Na^+, K^+-ATPase, *Biochim. Biophys. Acta 1105*, 51−60.
19. Bertagnolli, B. L., and Cook, P. F. (1994) Lanthanide Pyrophosphates as Substrates for the Pyrophosphate-Dependent Phosphofructokinases from *Propionibacterium freudenreichii* and *Phaseolus aureus*. Evidence for a Second Metal Ion Required for Reaction, *Biochemistry 33*, 1663−1667.
20. Fersht, A. (1977) *Enzyme Structure and Mechanism*, W. H. Freeman and Co., San Francisco, CA.
21. Payne, M. A., Rao, G. S. J., Harris, B. G., and Cook, P. F. (1995) Acid−Base Catalytic Mechanism and pH Dependence of Fructose 2,6-Bisphosphate Activation of the *Ascaris suum* Phosphofructokinase. *Biochemistry 34*, 7781−7787.
22. Armstrong, R. N., Kondo, H., Granot, J., Kaiser, E. T., and Mildvan, A. S. (1979) Magnetic Resonance and Kinetic Studies of the Manganese(II) Ion and Substrate Complexes of the Catalytic Subunit of Adenosine 3′,5′-Monophosphate Dependent Protein Kinase from Bovine Heart, *Biochemistry 18*, 1230−1238.
23. Donahue, M. J., Yacoub, H. M., Kaeini, M. R., Masaracchia, R. A., and Harris, B. G. (1981) Glycogen Metabolizing Enzymes During Starvation and Feeding of *Ascaris suum* Maintained in a Perfusion Chamber, *J. Parisitol. 67*, 505−510.

BI052191U